Inorg. Chem. **2008**, *47*, 12040−12048

Organozinc Aminoalcoholates: Synthesis, Structure, and Materials Chemistry

Andrew L. Johnson, Nathan Hollingsworth, Gabriele Kociok-Köhn, and Kieran C. Molloy*

Department of Chemistry, University of Bath, Claverton Down, Bath, BA2 7AY, U.K.

Received August 21, 2008

A series of novel organozinc aminoalcoholates have been synthesized by the reaction of the amino alcohols $HOCH_x(CH_2NMe_2)_{3-x}$ (x = 2, Hdmae; 1, Hbdmap; 0, Htdmap) with R_2Zn (R = Me, Et). The 1:1 reaction with Hdmae leads to the tetramers $[RZn(dmae)]_4$ [R = Me (**1**), Et (**2**)], while with Htdmap, dimeric $[RZn(tdmap)]_2$ [R = Me (**7**), Et (**8**)] are produced. Reaction with Hbdmap only yields $[MeZn(bdmap)]_n$ (**3**), an oil which mass spectral data suggests contains a mixture of Zn_2 - Zn_7 species, when a 2-fold excess of ligand is used. Crystals of dimeric $[Zn(bdmap)_2 \cdot Hbdmap]_2$ (**4**) deposit from this oil on prolonged standing. Reaction of Et_2Zn with Hbdmap (1:1) affords $[EtZn(bdmap)]_n$ (**5**), also an oil made up of Zn_3 and Zn_4 clusters on the basis of mass spectral evidence. Crystals of $EtZn_3(bdmap)_5$ (**6**) are formed within the oil that is **5** on standing. $[MeZn(tdmap)]_2$ (**7**) has been used as a single-source precursor for hexagonal ZnO films under low pressure chemical vapor deposition (LPCVD) conditions and a substrate temperature of 500 °C.

Introduction

Zinc oxide (ZnO) is one of the most widely studied metal oxides. In addition to its inherent ability to catalyze reactions such as the conversion of water gas to methanol[1] and the dehydrogenation of *sec*-butanol to methyl(ethyl)ketone,[2] it has an enormous variety of applications in the field of microelectronics. One of the hardest known members of the 12−16 family of semiconductors, ZnO has a band gap of 3.3 eV making it transparent to the majority of the solar spectrum. It is intrinsically an n-type semiconductor due to oxygen vacancies and zinc interstitials, but can be doped, for example, with Li, to afford p-type materials. Overall, it has a unique combination of piezoelectric, conducting, thermal and optical properties which have led to a plethora of applications, such as piezoelectric transducers, optical waveguides, gas sensors, solar cells, and surface acoustic wave devices to name but a selection.[3] Future applications of this important transparent conducting oxide (TCO) are in "invisible electronics"[4] and, as a diluted magnetic semiconductor (by doping with Mn^{2+}), in the emerging field of quantum computers (spintronics).[5]

Approaches to the deposition of ZnO thin films include *inter alia* spray pyrolysis, sputtering, pulsed laser deposition (PLD), atomic layer deposition (ALD), though metal-organic chemical vapor deposition (MOCVD) offers arguably the best opportunities for fast, conformal growth over a large area with good thickness control. Several single-source precursors (SSP) have been assessed for this latter technique, including $Zn(O_2CMe)_2$,[6,7] $Zn_4O(O_2CNEt_2)_6$,[8] the TMEDA adduct of zinc bis(2-thenoyl trifluoroacetonate),[9] $Zn[O_2CCHN(OMe)]_2 \cdot 2H_2O$,[10] and various β-diketonates,[11]

* To whom correspondence should be addressed. E-mail: k.c.molloy@bath.ac.uk.

(1) Spencer, M. S. *Catal. Lett.* **1998**, *50*, 37.
(2) Perez-Lopez, O. W.; Farias, A. C.; Marcilio, N. R.; Bueno, J. M. C. *Mater. Res. Bull.* **2005**, *40*, 2089.
(3) Triboulet, R.; Perriere, J. *Prog. Cryst. Growth Charact. Mater.* **2003**, *47*, 64.
(4) Banerjee, A. N.; Chattopadhyay, K. K. *Prog. Cryst. Growth Charact. Mater.* **2005**, *50*, 52.
(5) Che Mofor, A.; El-Shaer, A.; Bakin, A.; Wehmann, H.-H.; Ahlers, H.; Siegner, U.; Sievers, S.; Albrecht, M.; Schoch, W.; Izyumskaya, N.; Avrutin, V.; Stoemenos; J, A; Waag, A. *Superlattices Microstruct.* **2006**, *39*, 381.
(6) Mar, G. L.; Timbrell, P. Y.; Lamb, R. N. *Chem. Mater.* **1995**, *7*, 1890.
(7) Jain, S.; Kodas, T. T.; Hampden-Smith, M. *Chem. Vapor Deposition* **1998**, *4*, 51.
(8) Petrella, A. J.; Deng, H.; Roberrs, N. K.; Lamb, R. N. *Chem. Mater.* **2002**, *14*, 4339.
(9) Malandrino, G.; Blandino, M.; Perdicaro, L. M. S.; Fragala, I. L.; Rossi, P.; Dapporto, P. *Inorg. Chem.* **2005**, *44*, 9684.
(10) Hill, M. R.; Jomes, A. W.; Russell, J. J.; Roberts, N. K.; Lamb, R. N. *Inorg. Chim. Acta* **2005**, *358*, 201.
(11) Sato, H.; Minami, T.; Miyata, T.; Takata, S.; Ishii, M. *Thin Solid Films* **1994**, *246*, 65.

10.1021/ic801591d CCC: $40.75
Published on Web 11/13/2008

β-ketoiminates, and β-iminoesterates.[12] However, the most common approach has been a dual-source route involving R_2Zn and an oxygen source, commonly an alcohol. The epitaxial growth of ZnO films has been reviewed relatively recently, and includes an overview of both experimental methodology and precursor combinations.[3] In view of the importance of R_2Zn/ROH precursor combinations in this area of materials chemistry and the supposition that this deposition process involves organozinc alkoxides (RZnOR′) as intermediates, these organometallics themselves have been the focus of studies, both as SSPs in their own right[13,14] and from a more fundamental structural perspective. Such $(RZnOR')_n$ most commonly adopt tetrameric heterocubane structures ($n = 4$),[15−22] though dimers ($n = 2$)[17,23−27] are also prevalent particularly when steric bulk at either zinc or oxygen is increased. Less common are cyclic tetramers[28,29] and cyclic trimers ($n = 3$)[30] and variations on the cubane, for example, vertex-shared *bis*-cubanes[15,17,31,32] and face-sharing cubanes with two vertices missing.[31]

In view of the importance of molecular nuclearity in influencing key properties such as volatility and decomposition pathway, attempts have been made to saturate the metal coordination sphere with suitably disposed pendant donor groups as part of the alkoxide ligand, though the motivation for the work has usually been to develop chiral zinc alkoxides for asymmetric catalysis. These organozinc alkoxides are typically variations on the following themes (Scheme 1), with changes in the substituents on either the α-carbon and/or

Scheme 1

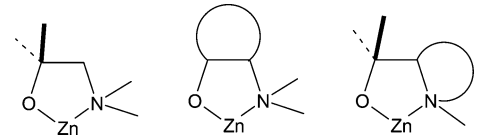

nitrogen, and/or the nature and location of the fused ring (e.g., pyrollidine, isobornene); both dimeric[25,30,33−35] and trimeric[30,36] products have been identified.

More recently, this interest has been expanded to included multifunctionalized donor sets, for example, O,N,N[37−39] and O,N,O,[40] based on amino-functionalized phenols of varying degrees of steric hindrance, and which favor dimers and even monomers.

In addition to the intrinsic structural nature of such studies, there is also a materials chemistry motivation for such work. That is, any uncoordinated donors can potentially be exploited to coordinate further metals and thus generate SSPs to more complex binary oxides, though to date in the case of zinc this appears to be limited to the use of $[ZnGa_2(OC_2H_4OMe)_8]_2$ for the formation of $ZnGa_2O_4$ by a sol−gel route.[41] $Fe_2Zn(OR)_8$ (R = ^{t}Bu, ^{i}Pr), though lacking donor functionalized alkoxides, has also been successfully employed to form $ZnFe_2O_4$, again by a sol−gel method.[42]

In light of the above and our own interest in the exploitation of flexible donor functionalized aminoalcohols **I**−**III** (dimethylaminoethanol, Hdmae; 1,3-*bis*-(dimethylamino)-propan-2-ol, Hbdmap; 1,3-*bis*(dimethylamino)-2-(dimethylaminomethyl)-propan-2-ol, Htdmap)[43,44] we have explored the reactions of these ligands with R_2Zn (R = Me, Et) and now report on the structural chemistry of the reaction products and an initial evaluation of their potential for the formation of zinc oxide materials.

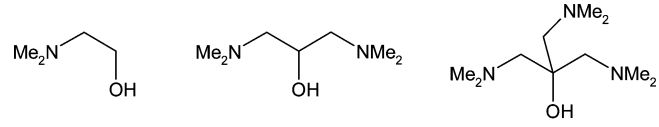

I : Hdmae **II** : Hbdmap **III**: Htdmap

Experimental Section

General Procedures. Elemental analyses were performed using an Exeter Analytical CE 440 analyzer. ^{1}H and ^{13}C NMR spectra

(12) Matthews, J. S.; Onakoya, O. O.; Ouattara, T. S.; Butcher, R. J. *Dalton Trans.* **2006**, 3806.
(13) Auld, J.; Houlton, D. J.; Jones, A. C.; Rushworth, S. A.; Malik, M. A.; O'Brien, P.; Critchlow, G. W. *J. Mater. Chem.* **1994**, *4*, 1249.
(14) Hambrock, J.; Rabe, S.; Merz, K.; Birkner, A.; Wohlfart, A.; Fischer, R. A.; Driess, M. *J. Mater. Chem.* **2003**, *13*, 1731.
(15) Jana, S.; Berger, R. J. F.; Fröhlich, R.; Pape, T.; Mitzel, N. W. *Inorg. Chem.* **2007**, *46*, 4293.
(16) Polarz, S.; Roy, A.; Merz, M.; Halm, S.; Schröder, D.; Schneider, L.; Bacher, G.; Kruis, F. E.; Driess, M. *Small* **2005**, *1*, 540.
(17) Boyle, T. J.; Bunge, S. D.; Andrews, N. L.; Matzen, L. E.; Sieg, K.; Rodriguez, M. A.; Headley, T. J. *Chem. Mater.* **2004**, *16*, 3279.
(18) Bond, A. D.; Linton, D. J.; Wheatley, A. E. H. *Acta Crystallogr., Sect. E* **2001**, *57*, m298.
(19) Driess, M.; Merz, K.; Rell, S. *Eur. J. Chem.* **2000**, 2517.
(20) Herrmann, W. A.; Bogdanovic, S.; Behm, J.; Denk, M. *J. Organomet. Chem.* **1992**, *430*, C33.
(21) Shearer, H. M. M.; Spencer, C. B. *Acta Crystallogr., Sect. B* **1980**, *36*, 2046.
(22) Shearer, H. M. M.; Spencer, C. B. *Chem. Commun.* **1966**, 194.
(23) Chisholm, M. H.; Gallucci, J. C.; Yin, H.; Zhen, H. *Inorg. Chem.* **2005**, *44*, 4777.
(24) Cole, S. C.; Coles, M. P.; Hitchcock, P. B. *Organometallics* **2004**, *23*, 5159.
(25) Nakano, K.; Nozaki, K.; Hiyama, T. *J. Am. Chem. Soc.* **2003**, *125*, 5501.
(26) Olmstead, M. M.; Power, P. P; Shoner, S. C. *J. Am. Chem. Soc.* **1991**, *113*, 3379.
(27) Parvez, M.; BergStresser, G. L.; Richey, H. G., Jr. *Acta Crystallogr., C* **1992**, *48*, 641.
(28) van der Schaaf, P. A.; Wissing, E.; Boersma, J.; Smeets, W. J. J.; Spek, A. L.; van Koten, G. *Organometallics* **1993**, *12*, 3624.
(29) Steen, F. H. v. d.; Boersma, J.; .Spek, A. L.; Koten, G. v. *Organometallics* **1991**, *10*, 2467.
(30) Hecht, E. *Z. Anorg. Allg. Chem.* **2000**, *626*, 2223.
(31) Lewinski, J.; Marciniak, W.; Lipkowski, J.; Justyniak, I. *J. Am. Chem. Soc.* **2003**, *125*, 12698.
(32) Ziegler, M. L.; Weiss, J. *Angew. Chem., Int. Ed.* **1970**, *9*, 905.
(33) Nakano, K.; Hiyama, T.; Nozaki, K. *Chem. Commun.* **2005**, 1871.
(34) Kitamura, M.; Okada, S.; Suga, S.; Noyori, R. *J. Am. Chem. Soc.* **1989**, *111*, 4028.
(35) Kitamura, M.; Suga, S.; Niwa, M.; Noyori, R. *J. Am. Chem. Soc.* **1995**, *117*, 4832.
(36) Hunger, J.; Blaurock, S.; Sieler, J. *Z. Anorg. Allg. Chem.* **2005**, *631*, 472.
(37) Cox, A. R. F.; Gibson, V. C; Marshall, E. L; White, A.J. P; Yeldon, D. *Dalton Trans.* **2006**, 5014.
(38) Williams, C. K.; Breyfogle, L. E.; Choi, S. K.; Nam, W.; Junior, V. G. Y.; Hillmyer, M. A.; Tolman, W. B. *J. Am. Chem. Soc.* **2003**, *125*, 11350.
(39) Corey, E. J.; Yuen, P.-W.; Hannon, F. J; Wierda, D. A. *J. Org. Chem.* **1990**, *55*, 784.
(40) Groysman, S.; Sergeeva, E; Goldberg, I; Kol, M. *Eur. J. Inorg. Chem.* **2006**, 2739.
(41) Daniele, S.; Tcheboukov, D.; Hubert-Pfalzgraf, L. G. *J. Mater. Chem.* **2002**, *12*, 2519.
(42) Veith, M.; Haas, M.; Huch, V. *Chem. Mater.* **2005**, *17*, 95.
(43) Hollingsworth, N.; Horley, G. A.; Mazhar, M.; Mahon, M. F.; Molloy, K. C.; Haycock, P. H.; Myers, C. P.; Critchlow, G. W. *Appl. Organomet. Chem.* **2006**, *20*, 687.
(44) Johnson, A. L.; Hollingsworth, N.; Kociok-Köhn, G.; Molloy, K. C. *Inorg. Chem.* **2008**, *47*, 9706.

were recorded on a Bruker Advance 300 or 500 MHz FT-NMR spectrometers, as appropriate, as saturated solutions at room temperature, unless stated otherwise; chemical shifts are in ppm with respect to Me_4Si, coupling constants are in Hz. SEM was carried out on a JEOL JSM-6310 microscope equipped with Oxford Instruments ISIS EDXS attachment. XRD was performed using a Bruker D8 diffractometer on which coupled $\theta-2\theta$ scans were carried out. A micrOTOFQ electrospray quadrupole time-of-flight (ESI-QTOF) mass spectrometer (Bruker Daltonik GmbH, Bremen, Germany) was used to determine the molecular mass of selected compounds. This was coupled to a syringe driver (Hamilton, Bonaduz, Switzerland) and the sample dissolved in CH_2Cl_2 and infused at a rate of 3 μL min^{-1}. TGA analyses were performed on a Perkin-Elmer TGA7 analyzer; samples were loaded as quickly as possible from a Schlenk tube under a rapid dry N_2 flow, then the temperature increased at a rate of 5 °C min^{-1} under a 0.02 L min^{-1} flow of N_2 gas.

All reactions were carried out under an inert atmosphere using standard Schlenk techniques. Solvents were dried and degassed under an argon atmosphere over activated alumina columns using an Innovative Technology solvent purification system (SPS).

Syntheses. Hdmae was purchased from Aldrich. Hbdmap[45] and Htdmap[46,47] were prepared by literature methods. The preparation of **III** used a 30% excess of perbenzoic acid in chloroform at *ca.* 60 °C over a period of at least one week to achieve nearly quantitative yields.

Synthesis of [MeZn(dmae)]$_4$ (1). Dimethylzinc (2 mL, 2.0 M solution in hexane, 4.0 mmol) was added to hexane (20 mL) and the solution was cooled to −78 °C. To this mixture Hdmae (0.39 g, 4.4 mmol) was added with stirring. After 1 h the mixture was allowed to warm to room temperature, whereby a white precipitate appeared which was redissolved by heating to 90 °C. Cooling to room temperature gave large colorless crystals (1.20 g, 44%, mp 233 °C dec). Analysis, found (calc for $C_5H_{13}NOZn$): C 35.7 (35.6), H 7.90 (7.77), N 8.33 (8.31)%. ^{1}H NMR (300 MHz, benzene-d_6): 3.79 (bs, 8H, OCH_2), 2.51 (bs, 8H, (CH_2N), 2.36 (s, 24H, N(CH_3)$_2$), −1.01 (s, 9H, CH_3Zn), −1.04 (s, 3H, CH_3Zn). ^{13}C NMR (300 MHz, benzene-d_6): 61.3 (CO), 59.7 (CH_2N), 43.3 (CH_3N), −20.3 (CH_3Zn).

Synthesis of [EtZn(dmae)]$_4$ (2). Diethylzinc (2 mL, 1.0 M solution in hexane, 2.0 mmol) was added to hexane (20 mL) and the solution was cooled to −78 °C. To this mixture Hdmae (0.20 g, 2.2 mmol) was added with stirring. After 1 h the mixture was allowed to warm to room temperature whereby a white precipitate appeared, which was redissolved by heating to 90 °C. Cooling to room temperature and reducing the volume of hexane gave colorless crystals (0.93 g, 59%, mp 105 °C). Analysis, found (calc for $C_6H_{15}NOZn$): C 39.8 (39.5), H 8.18 (8.28), N 7.78 (7.67)%. ^{1}H NMR (300 MHz, $CDCl_3$): 3.70 (bs, 8H, OCH_2), 2.38 (bs, 8H, (CH_2N), 2.29 (s, 24H, N(CH_3)$_2$), 1.10 (t, ^3J = 8.4, 12H, CH_3CH$_2$Zn), −0.10 (q, ^3J = 8.4, 8H, CH_2Zn). ^{13}C NMR (300 MHz, $CDCl_3$): 62.7 (CO), 60.2 (CH_2N), 44.7 (CH_3N), 12.6 (*C*H$_3$CH$_2$Zn), −4.5 (CH_2Zn).

Synthesis of [MeZn(bdmap)]$_3$ (3). Dimethylzinc (2 mL, 2.0 M solution in hexane, 4.0 mmol) was added to hexane (20 mL) and the solution was cooled to −78 °C. To this mixture Hbdmap (1.42 mL, 8.8 mmol) was added with stirring. The mixture was allowed to warm to room temperature whereby no precipitate appeared, stirring then commenced for 1 h, the mixture was then stirred at 65 °C for a further hour. Removal of the hexane yielded a clear oil; addition of a further 10 mL of hexane and its subsequent removal in vacuo followed by pumping for 6 h led to a more viscous clear oil. (1.52 g, 84%). Analysis found (calc for $C_8H_{20}N_2OZn$): C 42.9 (42.6), H 7.90 (8.93), N 12.8 (12.4)%. ^{1}H NMR (500 MHz, toluene-d_8): 3.76 (m, 3H, OCH), 2.17 (dd, ^{2}J 11.7, ^{3}J 8.2, 6H, CH_2N), 1.98 (bs, 24H, N(CH_3)$_2$), 1.97 (bs, 12H, N(CH_3)$_2$), 1.92 (dd, ^{2}J 11.7, ^{3}J 4.9, 6H, CH_2N), −0.89 (s, 9H, $ZnCH_3$). ^{13}C NMR (500 MHz, toluene-d_8): 68.6 (CO), 67.2 (CH_2N), 66.8 (CH_2N), 66.5 (CH_2N), 46.1 (CH_3N), −15.3 (CH_3Zn).

On prolonged storage in a refrigerator over several months, small crystals appeared in the oil which were identified crystallographically as [Zn(bdmap)$_2$·Hbdmap]$_2$ (**4**). No further characterization of this compound was made.

Synthesis of [EtZn(bdmap)]$_3$ (5). Diethylzinc (4 mL, 1.0 M solution in hexane, 4.0 mmol) was added to hexane (20 mL) and the solution was cooled to −78 °C. To this mixture Hbdmap (0.72 mL, 4.4 mmol) was added with stirring. The mixture was allowed to warm to room temperature and the hexane was removed, leaving a colorless oil (0.89 g, 93%). Analysis found (calc for $C_8H_{20}N_2OZn$): C 45.6 (45.1), H 9.17 (9.25), N 12.1 (11.7)%. ^{1}H NMR (500 MHz, toluene-d_8): 3.83 (m, 1H, OCH), 3.76 (m, 2H, OCH), 2.23 (m, 2H, CH_2N), 2.17 (m, 2H, CH_2N), 2.05 (m, 8H, CH_2N), 1.99 (s, 12H, N(CH_3)$_2$), 1.93 (s, 12H, N(CH_3)$_2$), 1.90 (s, 12H, N(CH_3)$_2$), 1.35 (m, 9H, C*H*$_3$CH$_2$Zn), 0.14 (m, 6H, CH$_3$C*H*$_2$Zn). ^{13}C NMR (500 MHz, toluene-d_8): 68.7 (OCH), 67.6 (CH_2N), 67.5 (CH_2N), 46.4 (CH_3N), 46.1 (CH_3N), 45.9 (CH_3N), 14.3 (*C*H$_3$CH$_2$Zn), 13.9 (*C*H$_3$CH$_2$Zn), 13.7 (*C*H$_3$CH$_2$Zn), −2.0 (CH$_3$*C*H$_2$Zn). ^{1}H NMR (500 MHz, toluene-d_8, 328 K), 500 MHz: 3.77 (br s, 1H, OCH), 2.14 (br s, 4H, CH_2N), 2.05 (br s, 8H, CH_2N), 1.95 (br s, 36H, N(CH_3)$_2$), 1.31 (br t, 9H, C*H*$_3$CH$_2$Zn), 0.13 (br q, 6H, CH$_3$C*H*$_2$Zn).

Standing for several months at room temperature afforded some colorless crystals embedded in the oil which were identified as $EtZn_3$(bdmap)$_5$ (**6**) by X-ray crystallography. ^{1}H NMR (300 MHz, benzene-d_6): 3.57 (br m, 5H, OCH), 2.04 (dd, ^2J 2.2, ^3J 8.2, 10H, CH_2N), 1.93 (dd, ^2J 12.2, ^3J 4.2, 10H, CH_2N), 1.81 (br s, 60H, N(CH_3)$_2$), 1.39 (t, ^3J 8.0, 3H, C*H*$_3$CH$_2$Zn), 0.24 (q, ^3J 8.0, 2H, CH$_3$C*H*$_2$Zn).

Synthesis of [MeZn(tdmap)]$_2$ (7). Dimethylzinc (2 mL, 2.0 M solution in hexane, 4.0 mmol) was added to hexane (20 mL) and the solution was cooled to −78 °C. To this mixture Htdmap (0.89 g, 4.4 mmol) was added with stirring. After 1 h the mixture was allowed to warm to room temperature whereby a white precipitate appeared, which was redissolved by heating to 70 °C. Cooling to room temperature gave large colorless cube-shaped crystals (2.03 g, 90%, mp 173 °C). Analysis, found (calc for $C_{11}H_{27}N_3OZn$): C 46.8 (46.7), H 9.52 (9.63), N 14.9 (14.9)%. ^{1}H NMR (500 MHz, toluene-d_8): 2.58 (s, 12H, CH_2N), 2.30 (s, 36H, (N(CH_3)$_2$), −0.28 (s, 6H, CH_3Zn). ^{13}C NMR (500 MHz, toluene-d_8): 77.6 (CO), 66.4 (CH_2N), 47.2 (CH_3N), −12.3 (CH_3Zn). Mass spectrum: observed 360.0961, calculated for [M-tdmap] 360.0966.

Synthesis of [EtZn(tdmap)]$_2$ (8). Diethylzinc (2 mL, 1.0 M solution in hexane, 2.0 mmol) was added to hexane (20 mL) and the solution was cooled to −78 °C. To this mixture Htdmap (0.45 g, 2.2 mmol) was added with stirring. After 1 h the mixture was allowed to warm to room temperature whereby a white precipitate appeared which was redissolved by heating to 70 °C. Cooling to room temperature gave large colorless cube-shaped crystals (0.86 g, 72%, mp 147 °C). Analysis, found (calc for $C_{12}H_{29}N_3OZn$): C 46.6 (48.6), H 10.0 (9.85), N 14.1 (14.2)%. ^{1}H NMR (500 MHz, toluene-d_8): 2.57 (s, 12H, CH_2N), 2.31 (s, 36H, (N(CH_3)$_2$), 1.07 (t, ^{3}J = 8.2, 6H, CH_3CH$_2$Zn), 0.55 (q, ^3J = 8.2, 4H, CH_2Zn). ^{13}C

(45) Campbell, K. N.; LaForge, R. A.; Campbell, B. K. *J. Org. Chem.* **1949**, *14*, 346.
(46) Müller, G.; Schätzle, T. *Z. Naturforsch., B: Chem. Sci.* **2004**, *59*, 1400.
(47) Gasteiger, J.; Herzig, C. *J. Chem. Res., Synop.* **1981**, 113.

Table 1. Crystallographic Data for **1**, **2**, **4**, **6**−**8**

	(**1**)	(**2**)	(**4**)	(**6**)	(**7**)	(**8**)
formula	$C_{20}H_{52}N_4O_4Zn_4$	$C_{24}H_{60}N_4O_4Zn_4$	$C_{42}H_{99}N_{12}O_6Zn_2$	$C_{37}H_{90}N_{10}O_5Zn_3$	$C_{22}H_{54}N_6O_2Zn_2$	$C_{24}H_{58}N_6O_2Zn_2$
M_w	674.22	730.32	999.07	951.30	565.45	593.50
crystal system	tetragonal	monoclinic	triclinic	triclinic	monoclinic	triclinic
space group	$P4_2/n$	$P2_1/c$	$P\bar{1}$	$P\bar{1}$	$P2_1/n$	$P\bar{1}$
a (Å)	13.4542(1)	20.8790(2)	9.7476(2)	11.0851(3)	9.9080(1)	8.9180(4)
b (Å)	13.4542(1)	10.8090(1)	14.3518(3)	12.4696(3)	13.7230(2)	9.4400(4)
c (Å)	8.4337(1)	16.6740(1)	21.6129(6)	20.6063(7)	11.6420(1)	10.4490(5)
α (°)			103.020(1)	100.388(1)		105.527(2)
β (°)		111.877(1)°	90.159(1)	95.953(1)	113.276(1)	105.796(2)
γ (°)			101.215(2)	113.042(1)		102.533(2)
V (e Å^3)	1526.63(2)	3492.02(5)	2886.13(12)	2529.89(13)	1454.10(3)	774.66(6)
Z	2	4	2	2	2	1
ρ (calc) (mg m^3)	1.467	1.389	1.151	1.249	1.291	1.272
μ(Mo Kα) (mm^{-1})	3.133	2.745	0.880	1.456	1.677	1.577
F(000)	704	1536	1088	1024	608	320
crystal size (mm)	0.30 × 0.30 × 0.30	0.40 × 0.40 × 0.35	0.25 × 0.25 × 0.20	0.33 × 0.30 × 0.25	0.55 × 0.55 × 0.30	0.40 × 0.35 × 0.30
indept reflns [R(int)]	2229 [0.0364]	10198 [0.0400]	12526 [0.0807]	10971 [0.0399]	4231 [0.0333]	4030 [0.0428]
reflns obs [$I > 2\sigma(I)$]	1918	8459	6766	8469	3930	3032
max, min transn factors	0.736, 0.670	0.383, 0.334	0.844, 0.810	0.698, 0.632	0.602, 0.436	0.630, 0.554
goodness-of-fit	1.049	0.997	0.955	1.076	1.043	0.997
final $R1$, $wR2$ [$I > 2\sigma(I)$]	0.0255, 0.0613	0.0319, 0.0681	0.0506, 0.1107	0.0536, 0.1176	0.0235, 0.0604	0.0363, 0.0696
final $R1$, $wR2$ (all data)	0.0315, 0.0651	0.0436, 0.0723	0.1241, 0.1359	0.0765, 0.1296	0.0262, 0.0623	0.0635, 0.0758
largest peak, hole (e Å^3)	0.436, −0.603	0.311, −0.406	0.428, −0.493	0.708, −0.693	0.345, −0.419	0.403, −0.425

NMR (500 MHz, toluene-d_8): 77.0 (CO), 66.4 (CH_2N), 47.2 (CH_3N), 12.7 (CH_3CH_2Zn), 0.7 (CH_2Zn).

Crystal Structures. Experimental details relating to the single-crystal X-ray crystallographic studies are summarized in Table 1. For all structures, data were collected on a Nonius Kappa CCD diffracrometer at 150(2) K using Mo−Kα radiation (λ = 0.71073 Å). The structures were refined using full-matrix least-squares on F^2. All non-hydrogen atoms were refined anisotropically; hydrogen atoms were included at calculated positions except for the OH hydrogen of **4** which was located in the difference map and refined. Data for **2**, **4**, and **8** were corrected for absorption, and for **2** also for extinction effects.

In the case of EtZn(dmae) (**2**) Zn, OCH_2, the CH_2 groups of the ethyl functionalities exhibited 83:17 disorder. The CH_3 carbons of the ethyl groups [C(2), C(8), C(14), and C(20)] were uniformly treated as two partial atoms in the ratio above, with common coordinates. Hydrogen atoms were included at calculated positions, with those attached to -NCH_2 carbons (common to both disordered moieties) being included at two sites, each reflecting the optimized geometry for each contributing part.

In the structure of Zn(bdmap)$_2$·Hbdmap (**4**), the NMe_2 group based on N(6) was disordered over two positions for the methyl groups in 60:40 ratio, while the CH_2NMe_2 part based on N(1) was disordered for all three carbon atoms, each two over sites in a 50:50 ratio.

Crystallographic data for the structural analyses (in CIF format) have been deposited with the Cambridge Crystallographic Data Center, CCDC nos. 698985−698990 for (**1**), (**2**), (**4**), (**6**), (**7**), and (**8**), respectively. Copies of this information may be obtained from the Director, CCDC, 12 Union Road, Cambridge, CB21EZ, UK (Fax: +44-1233-336033; e-mail: deposit@ccdc.cam.ac.uk or www.ccdc.cam.ac.uk).

LPCVD Study. Films were deposited on a 76 × 26 × 1.0 mm microscope slide using a hot wall LPCVD reactor which has been described in detail elsewhere.[48] A total of 0.15 g of [MeZn(tdmap)]$_2$ (**7**) was heated to 110 °C in a tube furnace under a vacuum of *ca.* 0.1 mmHg; the glass substrate was heated to 500 °C and the run time was 1 h.

(48) Horley, G. A.; Mahon, M. F.; Molloy, K. C.; Haycock, P. W.; Myers, C. P. *Inorg. Chem.* **2002**, *41*, 5052.

Results and Discussion

Synthesis and Spectroscopy. Six new organozinc alkoxides have been synthesized by the reaction of R_2Zn (R = Me, Et) and the functionalized aminoalkoxides **I**−**III** in hexane at −78 °C. Warming to room temperature yielded white solids in the cases of **1**, **2**, **7**, and **8**, which redissolved on gentle heating forming solutions from which colorless crystals deposited on cooling. In analogous, but not identical, protocols ligand **II** generated oils (**3**, **5**).

$$R_2Zn + HOR' \xrightarrow[\text{hexane}]{\text{- HR}} [RZnOR']_x \qquad (1)$$

x	R = Me	R = Et
4	$CH_2CH_2NMe_2$ (**1**)	$CH_2CH_2NMe_2$ (**2**)
[a]	$CH(CH_2NMe_2)_2$ (**3**)	$CH(CH_2NMe_2)_2$ (**5**)
2	$C(CH_2NMe_2)_3$ (**7**)	$C(CH_2NMe_2)_3$ (**8**)

[a] unknown

In the cases of **1**, **2**, **7**, and **8** the stoichiometric reaction resulted in the anticipated liberation of 1 equivalent of alkane; more complex behavior was seen in the case of the Hbdmap ligand. All the compounds described above are air- and moisture-sensitive solids or oils, soluble in common organic solvents; yields were in the range 44−93%.

The structures of **1** and **2** are shown in Figures 1 and 2, respectively, and both adopt a folded tetrameric arrangement.

1 has crystallographic 4-fold symmetry while **2** not only lacks this symmetry but shows considerable structural disorder. Similar puckering of the eight-membered Zn_4O_4 ring has been noted for $Me_3SiCH_2ZnOCH_2C_5H_4N$-2,[28] and the zinc ester enolate EtZnOC(OMe)═C(H)N(Me)Bu^t.[29] The Zn−O bond lengths in **1** and **2** are indicative of a strong bridging interaction, with no marked differences between the formally covalent and dative Zn−O interactions. For **1** these are 1.9741(10) and 1.9754(10) Å, respectively, which both lie in the range of Zn−O interactions evident in **2** [1.9693(16)−1.9859(16) Å]. Both species have similarly strong dative N:→Zn bonds [**1**: 2.2086(13); **2**: 2.1861(19)−2.2078(18) Å].

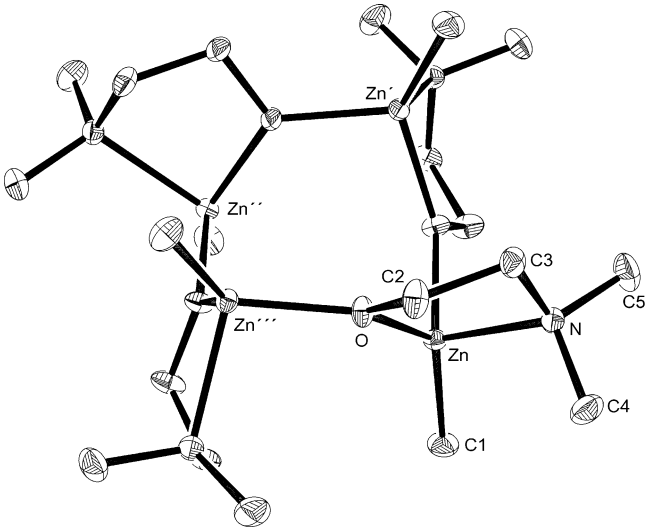

Figure 1. The tetrameric structure of **1**. The asymmetric unit containing one zinc is shown along with the labeling scheme used; thermal ellipsoids are at the 50% probability level. Selected bond lengths and angles: Zn−O 1.9754(10), Zn−O′ 1.9741(10), Zn−C(1) 1.9780(16), Zn−N 2.2086(13), O−C(2) 1.4098(18), C(2)−C(3) 1.518(2), N−C(3) 1.473(2), N−C(4) 1.467(2), N−C(5) 1.465(2) Å; O−Zn−O′ 100.82(5), O−Zn−C(1) 131.62(6), O−Zn−N 83.10(5), O′−Zn−C(1) 118.98(7), O′−Zn−N 98.94(5), C(1)−Zn−N 113.98(7), Zn−O−Zn′′′ 129.00(5), C(2)−O−Zn′′′ 116.85(9), C(2)−O−Zn 114.13(9)°. Symmetry operations: ′ *y*, 1/2 − *x*, 3/2 − *z*. ′′ 1/2 − *x*, 1/2 − *y*, *z*. ′′′ 1/2 − *y*, *x*, 3/2 − *z*.

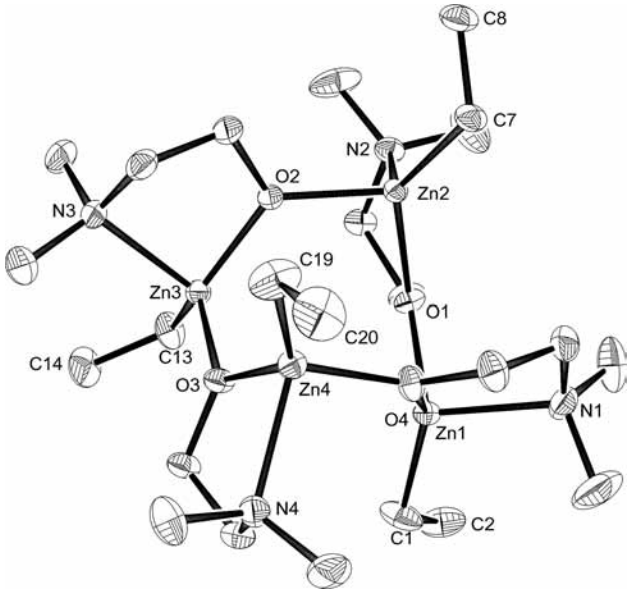

Figure 2. The asymmetric unit of **2** showing the labeling scheme used; thermal ellipsoids are at the 50% probability level. Only the major component of the disorder is shown for clarity. Selected bond lengths and angles for the environment of Zn(1), typical of all four metal centers: Zn(1)−O(1) 1.9769(15), Zn(1)−O(4) 1.9839(16), Zn(1)−N(1) 2.1867(18) Å; O(1)−Zn(1)−C(1) 121.94(11), C(1)−Zn(1)−O(4) 130.93(10), O(1)−Zn(1)−O(4) 99.29(7), C(1)−Zn(1)−N(1) 112.40(12), O(1)−Zn(1)−N(1) 99.21(7), O(4)−Zn(1)−N(1) 82.73(7)°.

The structures of these two puckered tetramers are most readily appreciated with respect to the more familiar heterocubane adopted by many organozinc alkoxides derived from purely monodentate alcohols, for example, [MeZn(OMe)]$_4$, which incorporates three identical (within error) Zn−O bonds [2.0647(19), 2.0673(18), 2.0690(19) Å].[18] The effect of the donor amine is to fulfill the tetrahedral

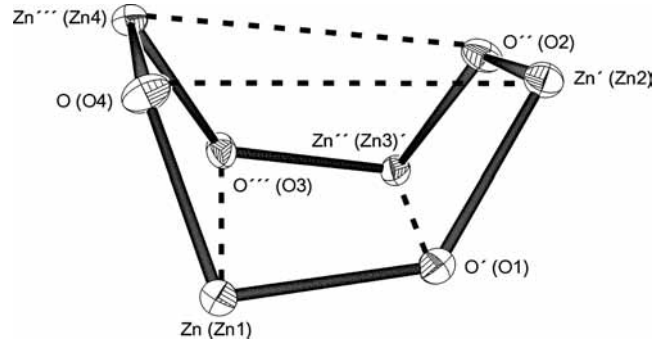

Figure 3. The Zn_4O_4 core of **1** and **2**; labeling for **1** is shown while that for **2** is given in parentheses. For **1**, all long interactions (e.g., Zn···O′′′) = 3.626 Å. For **2**: Zn(1)···O(3) 3.462, Zn(2)···O(4) 3.476, Zn(3)···O(1) 3.435, Zn(4)···O(2) 3.486 Å.

coordination about zinc without the need for a third O:→Zn linkage, which opens the cubane by effectively breaking four such interactions (Figure 3).

The ^{1}H NMR spectra of both **1** and **2** contain broad signals at room temperature. The spectrum of **1** is the simpler of the two, though even here the only signal resolution is in the MeZn region which shows two signals in a 3:1 ratio, though the implications of this are unclear. All other resonances are broad, though that of the NMe_2 protons sharpens in $CDCl_3$. As the sample of of **1** in toluene is cooled to 258 K, the NMR signals due to Me_2Zn protons become more resolved, appearing as a 1:1:2 set, which is matched by a resolution of the NMe_2 signals into analogous 1:1:2 singlets. These latter signals overlay a complex pattern associated with the CH_2N protons which in turn parallel a complex, though sharpened, set of signals at *ca.* 3.8 ppm due to OCH_2. To some extent the tetrameric structure (see above), though lacking crystallographic symmetry, becomes evident at lower temperatures.

The two tdmap derivatives (**7**, **8**) are dimers which incorporate tetrahedral zinc centers and a planar, central Zn_2O_2 core (Figures 4 and 5, respectively), similar to those reported by others for a variety of chiral aminoalcohols (Scheme 1),[25,30,33−35] and, in the case of **7**, iso-structural with its cadmium analogue.[44]

Each zinc has a $CZnO_2N$ coordination sphere comprising robust Zn−O [**7**: 2.0075(8), 2.0324(7); **8**: 2.0041(12), 2.0451(12) Å] and Zn−N [**7**: 2.1798(9); **8**: 2.1847(16) Å] interactions, though in comparison with **1**, **2** the Zn−O bonds have weakened slightly at the expense of stronger N:→Zn coordination. In both structures, each tdmap ligand embodies two uncoordinated tertiary amine groups which retain the capacity for further metal binding. The two hydrocarbon ligands are disposed in a *trans* manner with respect to the central Zn_2O_2 ring as are the two chelate rings, as would be anticipated on steric grounds. The ^{1}H NMR spectra of both **7** and **8** are unexceptional, save that they display a single environment for the ligand protons indicating rapid exchange of CH_2NMe_2 arms which are coordinated to zinc.

The reactions between Hbdmap (**II**) and R_2Zn are less straightforward. In the case of Me_2Zn, a 1:1 reaction stoichiometry causes only partial alkene elimination, and an excess of alcohol is required (1:2 stoichiometry) to form

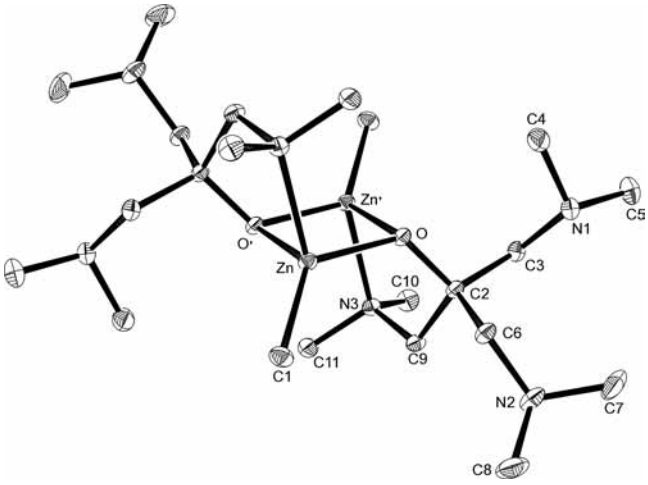

Figure 4. The dimeric structure of **7**. The asymmetric unit containing one zinc is shown along with the labeling scheme used; thermal ellipsoids are at the 50% probability level. Selected bond lengths and angles: Zn−C(1)1.9750(11), Zn−O 2.0075(8), Zn−O′ 2.0324(7), Zn−N(3′) 2.1798(9) Å; C(1)−Zn−O 129.00(4), C(1)−Zn−O′ 125.98(4), C(1)−Zn−N(3′) 120.37(5), O−Zn−O′ 86.67(3), O−Zn−N(3′) 99.22(3), O′−Zn−N(3′) 83.17(3) Zn−O−Zn′ 93.33(3), C(2)−O−Zn 124.40(6), C(2)−O−Zn′ 109.60(6)°. Symmetry transformation: $1 - x$, $1 - y$, $1 - z$.

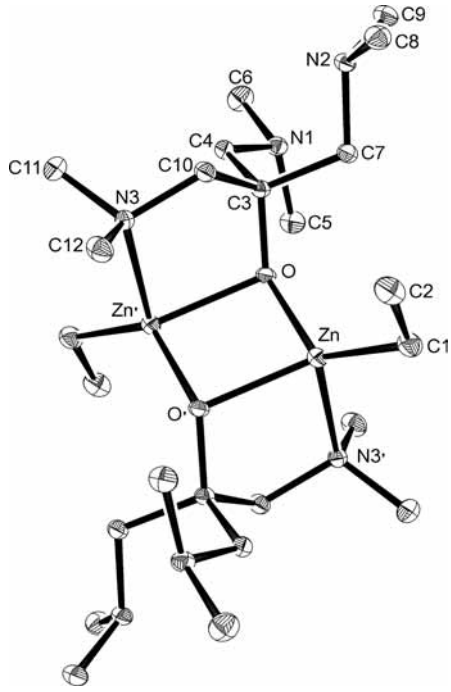

Figure 5. The dimeric structure of **8**. The asymmetric unit containing one zinc is shown along with the labeling scheme used; thermal ellipsoids are at the 50% probability level. Selected bond lengths and angles: Zn−C(1) 1.985(2), Zn−O 2.0041(12), Zn−O′ 2.0451(12), Zn−N(3′) 2.1847(16) Å; C(1)−Zn−O 130.74(7), C(1)−Zn−O′ 131.28(8), C(1)−Zn−N(3′) 114.05(8), O−Zn−O′ 85.28(5), O−Zn−N(3′) 100.31(6), O′−Zn−N(3′) 82.94(5), Zn−O−Zn′ 94.72(5), C(3)−O−Zn 125.26(11), C(3)−O−Zn′ 109.13(11)°. Symmetry transformation $2 - x$, $1 - y$, $1 - z$.

MeZn(bdmap) (**3**), which is an oil of unknown nuclearity. On prolonged storage at low temperature over several months, crystals of $[Zn(bdmap)_2 \cdot Hbdmap]_2$ (**4**) appeared within the oil which were identified crystallographically (see below). The formation of this homoleptic derivative is

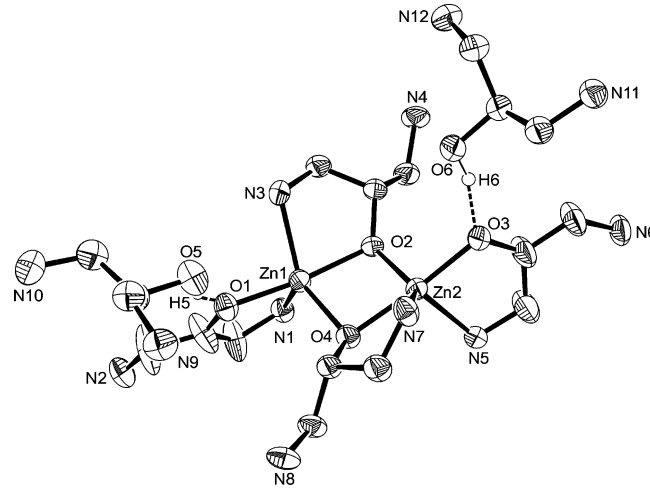

Figure 6. The asymmetric unit of **4** showing the labeling scheme used; thermal ellipsoids are at the 50% probability level. The two methyl groups on each nitrogen atom have been omitted for clarity. Selected bond lengths and angles are given in Table 2.

Table 2. Selected Bond Lengths and Angles for **4**[a]

Bond Lengths (Å)			
Zn(1)−O(1)	1.956(3)	Zn(1)−N(1)	2.176(3)
Zn(1)−O(2)	2.015(2)	Zn(1)−N(3)	2.239(3)
Zn(1)−O(4)	2.019(2)		
Bond Angles (°)			
O(1)−Zn(1)−O(2)	172.29(9)	O(2)−Zn(1)−N(1)	101.25(10)
O(1)−Zn(1)−O(4)	101.83(10)	O(2)−Zn(1)−N(3)	79.41(10)
O(1)−Zn(1)−N(1)	85.05(10)	O(4)−Zn(1)−N(1)	108.72(10)
O(1)−Zn(1)−N(3)	93.83(10)	O(4)−Zn(1)−N(3)	133.02(9)
O(2)−Zn(1)−O(4)	80.50(10)	N(1)−Zn(1)−N(3)	116.63(11)

[a] Only data for Zn(1) as typical of both metal environments is presented.

consistent with a Schlenk equilibrium between heteroleptic **3** and $Me_2Zn/Zn(bdmap)_2$, with some eventual crystallization of the latter coordinated by unreacted Hbdmap.

The spectral data for **3** are uninformative with regard to its structure. There are two environments for the NMe_2 protons in the ^1H NMR spectrum, while the mass spectrum shows fragments which have not been unambiguously assigned by have isotope distribution patterns typical of several Zn_x species ($x = 2-7$). The corresponding cadmium complex, MeCd(bdmap), is a trimer.[44]

Structure of $Zn(bdmap)_2 \cdot Hbdmap$ (**4**), which crystallizes from the oil that is **3** on prolonged standing, is shown in Figure 6 and selected structural data given in Table 2. The structure is dimeric, built around a central, slightly nonplanar Zn_2O_2 ring. Each zinc is five-coordinate by virtue of three oxygen and two nitrogen atoms. Both metals have distorted geometries between trigonal bipyramidal and square pyramidal, which a τ analysis[49] suggests is *ca.* 65% the former. On this basis, the axial ligands about Zn(1) are O(1) and O(2) [∠O(1)−Zn(1)−O(2) 172.29(9)°] and about Zn(2) are O(3), O(4) [∠O(3)−Zn(2)−O(4) 170.99(9)°]. The ligands fall into two pairs, one pair acting both as a μ_2-bridge between metals and an *O,N*-chelate [O(2), O(4)], while two are simply *O,N*-chelating [O(1), O(3)]; with all four ligands, one potentially ligating CH_2NMe_2 are remains coordinatively

(49) Addison, A. W.; Rao, T. N.; Reedijk, J.; van Rijn, J.; Verschoor, G. C. *J. Chem. Soc., Dalton Trans.* **1984**, 1349.

passive. The structure is completed by the hydrogen bonding of two Hbdmap molecules to the oxygen of each of the purely chelating ligands [H(5)···O(1) 1.77(6), O(1)···O(5) 2.617(4) Å, ∠O(5)−H(5)···O(1) 161(5)°, H(6)···O(3) 1.70(5), O(3)···O(6) 2.628(4) Å, ∠O(6)−H(6)···O(3) 165(5)°]. The Zn−O bonds to the bridging oxygen atoms are of comparable lengths to those involving the μ_2-oxygen atoms in **6**−**8** (*ca.* 2.01 Å) but longer than Zn−O bonds involving the μ_3-oxygen atoms in **1**, **2** (*ca.* 1.98 Å). The most remarkable Zn−O interactions involve O(1) and O(3), which are unusually short [1.957(2), 1.952(2) Å, respectively] in comparison with others in this report, particularly given that these oxygen atoms are also involved in hydrogen bonding. These distances reflect the enhanced Lewis acidity which the metals acquire by virtue of the presence of a stronger electron-withdrawing coordination sphere in comparison with the organozinc species described. The Zn−N bond lengths are unexceptional and are similar to those given earlier in this report.

The structure is similar to dimeric $Cd(tdmap)_2$, which also has two terminal *O*, *N*-chelating ligands, but which differs by incorporating two six-coordinate metals by virtue of the μ_2-O ligands each chelating both metal centers with pendant NMe_2 groups.[44]

In the case of Et_2Zn, a 1:1.1 reaction stoichiometry with Hbdmap also produces an oil whose microanalytical data and NMR spectra are, in contrast to the Me_2Zn reaction, consistent with the formation of EtZn(bdmap) (**5**). On prolonged standing, this oil deposits crystals identified as the unsymmetrical species $EtZn_3(bdmap)_5$ (**6**). As with **4**, the formation of **6** can also be rationalized in terms of Schlenk equilibria, with crystallization of **6** from a mix of species:

$$\begin{aligned} 2\underset{(5)}{EtZn(bdmap)} &\rightleftharpoons Et_2Zn + Zn(bdmap)_2 \\ 2Zn(bdmap)_2 + EtZn(bdmap) &\rightleftharpoons \underset{(6)}{EtZn_3(bdmap)_5} \end{aligned} \qquad (2)$$

The ^{1}H NMR spectrum of **5** at room temperature is suggestive of a trimeric species. The OCH protons appear in two environments (δ 3.83, 3.76 ppm) in 1:2 ratio, which separates into three equal signals at 218 K but which coalesce on heating to 328 K. Similarly, there are at least three environments for the CH_2 protons at 298 K (δ 2.23, 2.17, 2.05 ppm; 2:2:8) and three equally populated environments for the NMe_2 groups (δ 1.99, 1.93, 1.90 ppm). Two structures which are consistent with these data are (ethyl groups on zinc and methyl groups on nitrogen omitted for clarity):

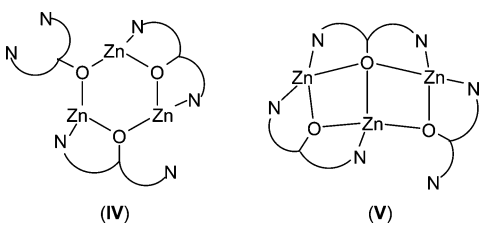

(**IV**) (**V**)

In **IV**, the CHO groups of the two chelating alkoxides might be expected to be similar, and differ from that of the purely bridging ligand. The four NMe_2 groups attached to the *bis*-chelating ligand would differ from the four which are totally uncoordinated, while the remaining four groups would appear equivalent if the two arms of the ligand are in a rapid on−off equilibrium. A similar reasoning would apply to **V**, although, as this involves zinc with a coordination number of five, it would seem less likely when viewed against the tetrahedral preference shown by other organozinc alkoxides. Cyclic RZn(OR′) trimers are rare but have been reported for other alkoxides systems,[30] while MeCd(bdmap) adopts structure **V**, though here the larger metal has a preference for higher coordination numbers.[44] The mass spectral data for **5**, however, suggest a more complex scenario, with fragments matching both Zn_3 and Zn_4 isotope distribution patterns identifiable.

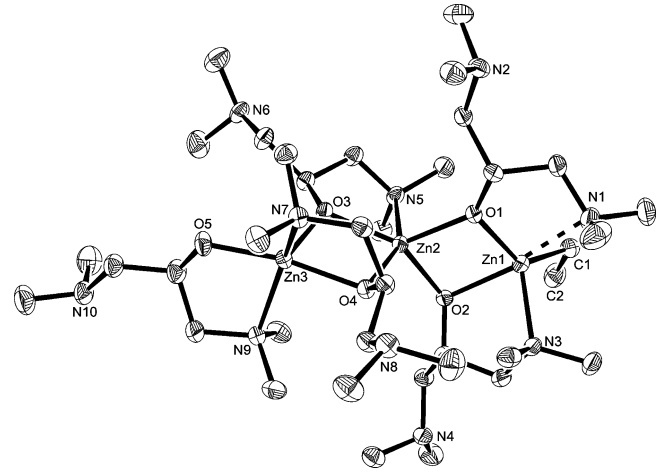

Figure 7. The asymmetric unit of **6** showing the labeling scheme used; thermal ellipsoids are at the 50% probability level. Selected bond lengths and angles are given in Table 3.

The structure of $EtZn_3(bdmap)_5$ (**6**) can be viewed as an aggregate of EtZn(bdmap) with two equivalents of Zn(bdmap)$_2$. The tri-zinc aggregate (Figure 7, Table 3) incorporates three five-coordinated centers, though each one is different. The one organozinc unit, Zn(1), has a $ZnCO_2N_2$ coordination sphere, though the donor bond from N(1) is very weak [2.804(4) Å] in comparison both with the structures described earlier and the N(3):→Zn(1) bond [2.161(3) Å] also present in **6**. Although the geometry about Zn(1) is suggested as predominantly square pyramidal by a τ analysis ($\tau = 0.22$)[49] in which N(1), O(2) and C(1), O(1) make up opposite pairs in the basal plane [O(2)−Zn(1)−N(1) 144.97(12), C(1)−Zn(1)−O(1) 131.53(15)°], of the three metal centers in this molecule Zn(1) shows the greatest distortion. The situation is probably better described in terms of distortion of a $ZnCO_2N$ tetrahedron, in which N(1) approaches zinc *trans* to O(2), which then weakens [2.161(3) Å] in comparison with Zn(1)−O(1) [1.989(3) Å]. The central Zn(2) is surrounded by four oxygens and a nitrogen, again in a distorted square pyramidal geometry ($\tau = 0.22$)[49] with O(4), N(5) and O(2), O(3) as opposites in the pyramid base [O(4)−Zn(2)−N(5) 154.93(11), O(2)−Zn(2)−O(3) 141.51(11)°]. This is also a heavily distorted geometry, with one particularly wide axial/basal angle for a square pyramidal description [O(1)−Zn(2)−O(3) 131.39 °]. The *trans*-coordination to N(5) renders Zn(2)−O(4) the weakest of the four Zn−O bonds to Zn(2) [2.071(3) *vs*

Table 3. Selected Bond Lengths and Angles for **6**

Bond Lengths (Å)

Zn(1)−C(1)	2.002(4)	Zn(2)−O(4)	2.071(3)
Zn(1)−O(1)	1.989(3)	Zn(2)−N(5)	2.373(3)
Zn(1)−O(2)	2.106(3)	Zn(3)−O(3)	1.987(2)
Zn(1)−N(3)	2.161(3)	Zn(3)−O(4)	2.056(3)
Zn(1)−N(1)	2.804(4)	Zn(3)−O(5)	1.929(3)
Zn(2)−O(1)	1.997(3)	Zn(3)−N(7)	2.173(3)
Zn(2)−O(2)	1.989(2)	Zn(3)−N(9)	2.229(3)
Zn(2)−O(3)	1.992(2)		

Bond Angles (°)

C(1)−Zn(1)−O(1)	131.53(15)	O(3)−Zn(2)−O(4)	79.58(10)
C(1)−Zn(1)−O(2)	117.51(16)	O(3)−Zn(2)−N(5)	77.09(10)
C(1)−Zn(1)−N(3)	113.24(16)	O(4)−Zn(2)−N(5)	154.93(11)
C(1)−Zn(1)−N(1)	97.35(17)	O(3)−Zn(3)−O(4)	80.05(10)
O(1)−Zn(1)−O(2)	82.02(10)	O(3)−Zn(2)−O(4)	113.44(12)
O(1)−Zn(1)−O(3)	113.57(12)	O(3)−Zn(3)−N(7)	104.84(12)
O(1)−Zn(1)−N(1)	71.54(11)	O(3)−Zn(3)−N(9)	107.63(12)
O(2)−Zn(1)−N(3)	80.58(11)	O(4)−Zn(3)−O(5)	166.48(12)
O(2)−Zn(1)−N(1)	144.97(12)	O(4)−Zn(3)−N(7)	83.55(11)
N(1)−Zn(1)−N(3)	89.19(13)	O(4)−Zn(3)−N(9)	93.42(11)
O(1)−Zn(2)−O(2)	84.84(10)	O(5)−Zn(3)−N(7)	91.78(12)
O(1)−Zn(2)−O(3)	131.39(11)	O(5)−Zn(3)−N(9)	83.43(12)
O(1)−Zn(2)−O(4)	106.48(11)	N(7)−Zn(3)−N(9)	146.34(13)
O(1)−Zn(2)−N(5)	97.49(12)	Zn(1)−O(1)−Zn(2)	98.18(11)
O(2)−Zn(2)−O(3)	141.51(11)	Zn(1)−O(2)−Zn(1)	94.70(10)
O(2)−Zn(2)−O(4)	104.87(10)	Zn(2)−O(3)−Zn(3)	102.27(11)
O(2)−Zn(2)−N(5)	86.80(11)	Zn(2)−O(4)−Zn(3)	97.30(10)

1.989(2)−1.997(3) Å]. Finally, Zn(3) is also at the center of a distorted ZnO_4N square-based pyramid ($\tau = 0.33$)[49] with N(7), N(9) and O(4), O(5) forming opposite basal pairs [N(7)−Zn(3)−N(9) 146.34(13), O(4)−Zn(3)−O(5) 166.48(12)°]. The two N:→Zn(3) donor bonds are the strongest within the molecule [Zn(3)−N(7): 2.173(3); Zn(3)−N(9) 2.229(3) Å]. The two Zn_2O_4 rings are planar and essentially orthogonal to each other [84.9°], while the bdmap ligands act in a tridentate μ_2-*O*, chelating *O*,*N* mode with the exception of the ligand based on O(5),N(9) which is purely chelating in nature.

Compound **6** is, as far as we are aware, unique. Other acyclic, heteroleptic tri-zinc alkoxides are of general formula $R_2Zn_3(OR')_4$, in which a central $Zn(OR')_2$ is flanked symmetrically by two $RZn(OR')$ moieties.[19,23,26,50] Moreover, the coordination numbers of the metals in $R_2Zn_3(OR')_4$ are either 3 or 4, depending on the steric demands of the substituents.

The ^{1}H NMR of **6** shows a series of signals which integrate as expected from the formula of the trimer, including the presence of only a single ethyl group. A broad signal for the OCH protons occurs at 3.57 ppm, so there is no distinction between the four ligands which bridge and chelate from the unique, chelate-only variant. While the CH_2 protons appear as two complex multiplets each integrating to 10 hydrogens, it is probably an oversimplification to suggest that these correspond directly to the five CH_2 groups of chelate rings and five which correspond to non-coordinated CH_2NMe_2 moieties, though this is possible. The appearance of a single, relatively sharp signal for the sixty NMe_2 protons must imply fluxionality at room temperature, with rapid interchange of chelating and free donor nitrogen centers.

(50) Merz, K.; Hu, H.-M.; Rell, S.; Driess, M. *Eur. J. Inorg. Chem.* **2003**, 51.

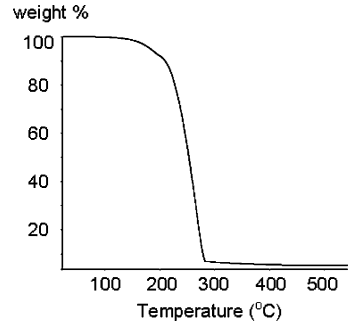

Figure 8. TGA of **7**.

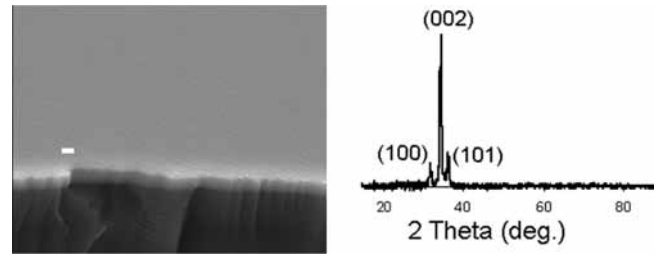

Figure 9. (a) SEM and (b) XRD of the film deposited from **7** by LPCVD at 500 °C. Bar = 1 μm. The XRD pattern is indexed to hexagonal zinc oxide PDF 79-0208.

CVD Studies. From the novel compounds reported herein, $[MeZn(tdmap)]_2$ (**7**) was selected for evaluation as a CVD precursor for the deposition of ZnO films. Compounds **1** and **2** based on the dmae ligand differ only marginally in structure from the cubane $[MeZnOMe]_4$ which have been used by others in this context,[13,14] while derivatives of Hbdmap (**3**, **5**) show complex Schlenk equilibria in solution which are likely to be replicated at elevated temperatures in the gas phase, complicating the deposition process. Of the compounds reported, those based on Htdmap (**7**, **8**) offer the lowest nuclearity (hence highest potential volatility) and rigid structural integrity.

TGA of **7** (Figure 8) shows that at atmospheric pressure sublimation begins at $T >$ *ca.* 150 °C leaving virtually no residue by 300 °C. These temperatures are a little lower than reported for other LPCVD precursors e.g. $Zn(tta)_2 \cdot TMEDA$ (tta = 2-thenoyl trifluoroacetonate).[9]

Although possible as a precursor for atmospheric pressure CVD, we have adopted a low pressure (0.1 mmHg) approach to minimize the precursor heating (110 °C). Although films could be deposited at substrate temperatures as low as 300 °C, a film of suitable thickness for analysis was grown at 500 °C over a period of 1 h. An SEM of the film (Figure 9a) shows it to be of smooth, rather than granular, texture and *ca.* 0.7 μm in thickness. EDXS of the film confirmed the presence of both zinc and oxygen, while the signal due to carbon suggests only trace amounts are present. The glancing-angle X-ray diffraction pattern from the film (Figure 9b) can be indexed to hexagonal ZnO with some preferred (002) orientation.

Conclusions

Reaction of ZnR_2 (R = Me, Et) with the aminoalkoxides Hdmae and Htdmap has led to the isolation of the oligomers $[RZn(dmae)]_4$ and $[RZn(tdmap)]_2$, respectively. The monoam-

inoalkoxide (dmae) fails to disrupt significantly the tetrameric cubane structure common among unfunctionalized $[RZnOR']_4$, though N:→Zn donation does result in a more open structure. The species based on the most functionalized ligand, the tris-aminoalkoxide Htdmap, have the lowest nuclearity (dimers), though this appears to accrue from the steric demands of the ligand as much as the presence of donor functions, as only one of three available amine groups bonds to the metal. This, however, offers opportunities for further complexation to form bimetallic alkoxides. The analogous reactions with Hbdmap are more complex, with MeZn(bdmap) only formed when an excess of Hbdmap is used. MeZn(bdmap) is an oil of unknown structure, but extrudes dimeric $Zn(bdmap)_2$ as an Hbdmap solvate on prolonged standing. EtZn(bdmap) is formed from 1:1 reaction of Et_2Zn with Hbdmap, and is also an oil but which affords crystals of the trimetallic species $EtZn_3(bdmap)_5$ over time. Thus, the structural chemistry of the bdmap series is the least well-defined in this report, though trimers appear to be common, as with the corresponding cadmium species, among a range of Zn_n clusters observed in the mass spectra. Among the compounds reported, $[MeZn(tdmap)]_2$ has the best combination of properties for CVD (low nuclearity hence good volatility, good structural integrity) and affords smooth films of ZnO under LPCVD conditions (precursor temperature 110 °C, substrate temperature 500 °C).

Acknowledgment. We thank the EPSRC for a doctoral training award (to N.H.) and for the purchase of the mass spectrometer. Mr. H. R. Perrot and Dr. A. Lubben (University of Bath) are thanked for help with the SEM, EDXS analyses of the thin film and mass spectral data, respectively. SAFC Hi-tech are thanked for a gift of Me_2Zn.

Supporting Information Available: Crystallographic information files (CIF) are available free of charge via the Internet at http://pubs.acs.org.

IC801591D